Expression of Alternatively Spliced Human T-Cell Leukemia Virus Type 1 mRNAs Is Influenced by Mitosis and by a Novel *cis*-Acting Regulatory Sequence

Ilaria Cavallari,[a] Francesca Rende,[a] Marion K. Bona,[b] Joanna Sztuba-Solinska,[c] Micol Silic-Benussi,[a] Martina Tognon,[a] Stuart F. J. LeGrice,[c] Genoveffa Franchini,[d] Donna M. D'Agostino,[e] Vincenzo Ciminale[a,f]

Department of Surgery, Oncology and Gastroenterology, University of Padua, Padua, Italy[a]; Leidos Biomedical Research, Inc., Frederick National Laboratory, Frederick, Maryland, USA[b]; Basic Research Laboratory, National Cancer Institute, Frederick, Maryland, USA[c]; Animal Models and Retroviral Vaccines Section, National Cancer Institute, Bethesda, Maryland, USA[d]; Department of Biomedical Sciences, University of Padua, Padua, Italy[e]; Istituto Oncologico Veneto-IRCCS, Padua, Italy[f]

ABSTRACT

Human T-cell leukemia virus type 1 (HTLV-1) expression depends on the concerted action of Tax, which drives transcription of the viral genome, and Rex, which favors expression of incompletely spliced mRNAs and determines a 2-phase temporal pattern of viral expression. In the present study, we investigated the Rex dependence of the complete set of alternatively spliced HTLV-1 mRNAs. Analyses of cells transfected with Rex–wild-type and Rex-knockout HTLV-1 molecular clones using splice site-specific quantitative reverse transcription (qRT)-PCR revealed that mRNAs encoding the p30Tof, p13, and p12/8 proteins were Rex dependent, while the *p21rex* mRNA was Rex independent. These findings provide a rational explanation for the intermediate-late temporal pattern of expression of the *p30tof*, *p13*, and *p12/8* mRNAs described in previous studies. All the Rex-dependent mRNAs contained a 75-nucleotide intronic region that increased the nuclear retention and degradation of a reporter mRNA in the absence of other viral sequences. Selective 2′-hydroxyl acylation analyzed by primer extension (SHAPE) analysis revealed that this sequence formed a stable hairpin structure. Cell cycle synchronization experiments indicated that mitosis partially bypasses the requirement for Rex to export Rex-dependent HTLV-1 transcripts. These findings indicate a link between the cycling properties of the host cell and the temporal pattern of viral expression/latency that might influence the ability of the virus to spread and evade the immune system.

IMPORTANCE

HTLV-1 is a complex retrovirus that causes two distinct pathologies termed adult T-cell leukemia/lymphoma and tropical spastic paraparesis/HTLV-1-associated myelopathy in about 5% of infected individuals. Expression of the virus depends on the concerted action of Tax, which drives transcription of the viral genome, and Rex, which favors expression of incompletely spliced mRNAs and determines a 2-phase temporal pattern of virus expression. The findings reported in this study revealed a novel *cis*-acting regulatory element and indicated that mitosis partially bypasses the requirement for Rex to export Rex-dependent HTLV-1 transcripts. Our results add a layer of complexity to the mechanisms controlling the expression of alternatively spliced HTLV-1 mRNAs and suggest a link between the cycling properties of the host cell and the temporal pattern of viral expression/latency that might influence the ability of the virus to spread and evade the immune system.

Human T-cell leukemia virus type 1 (HTLV-1) is the causative agent of adult T-cell leukemia-lymphoma (ATLL) (1) and tropical spastic paraparesis/HTLV-1-associated myelopathy (TSP/HAM) (2). Accumulating evidence also supports an association between HTLV-1 infection and a number of chronic inflammatory diseases, including uveitis, arthropathy, and infective dermatitis (3).

HTLV-1 produces many alternatively spliced transcripts coding for virion components and regulatory and accessory proteins (Fig. 1) (4). The *gag*, *pro*, and *pol* genes are expressed from the unspliced genomic RNA, and the *env* gene is expressed from a singly spliced mRNA. The transcriptional activator Tax and the posttranscriptional regulatory protein Rex are translated from a doubly spliced bicistronic mRNA (5). Other alternatively spliced mRNAs produce the accessory proteins p21Rex, p12/8, p13, and p30Tof (6–8) and three recently identified Rex isoforms named Rex$_a$, Rex$_b$, and Rex$_c$ (9). The *hbz* gene is expressed from minus-strand mRNAs transcribed from promoters at the 3′ end of the provirus (10–12).

In order to express this complex array of alternatively spliced mRNAs, HTLV-1 must override the cellular RNA-processing machinery that would otherwise eliminate intron-containing transcripts through splicing and degradation. This expression strategy involves both positive and negative *cis*-acting regulatory elements, relatively inefficient splice sites, and Rex, which binds to an RNA element termed the Rex-responsive element (RXRE), located at
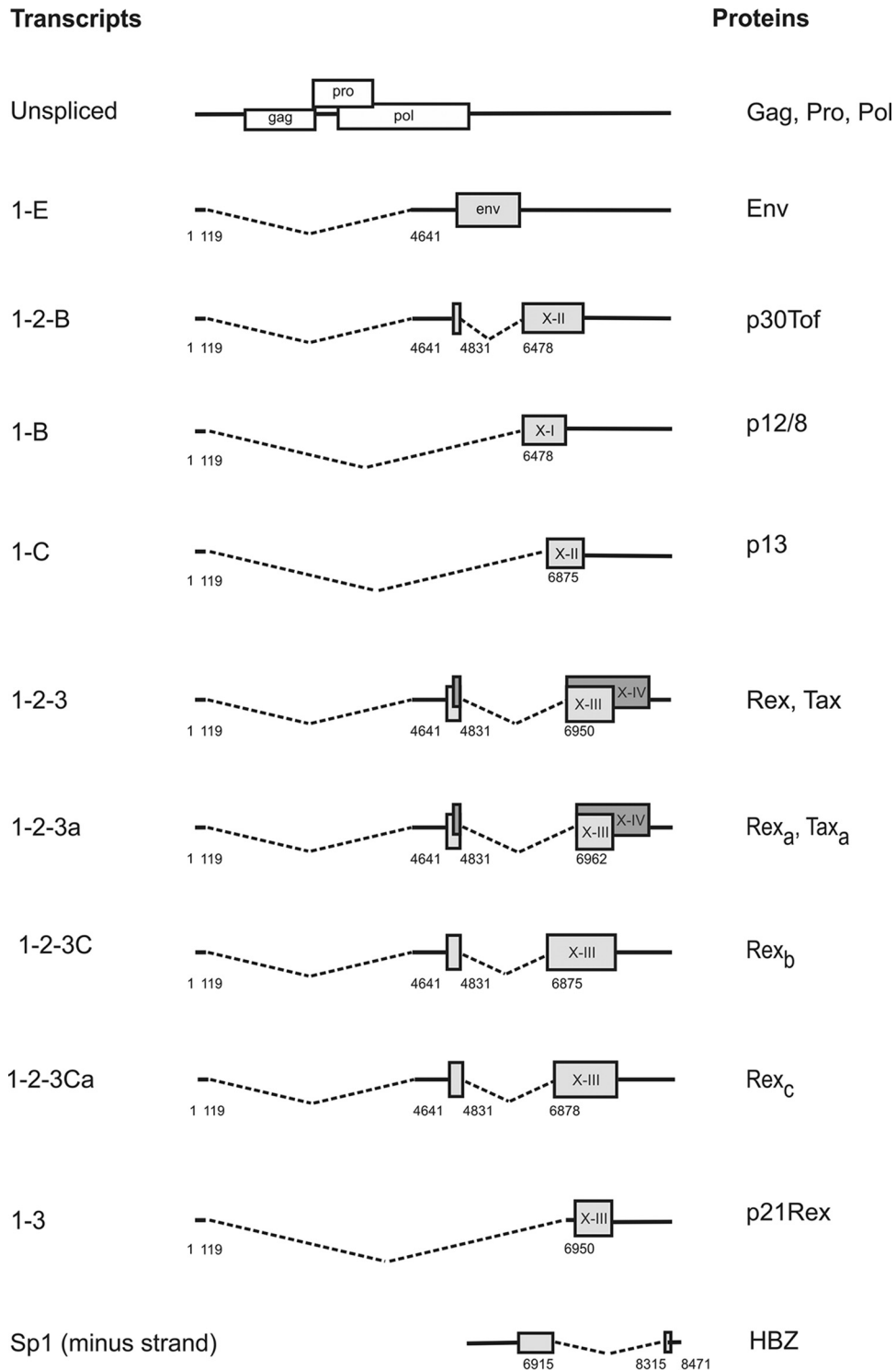
FIG 1 Genetic organizations and alternative splicing patterns of HTLV-1 mRNAs. The exon composition and coding potential of HTLV-1 alternatively spliced mRNAs are presented. Open reading frames (ORFs) are indicated by boxes. Splice sites are indicated by numbers. Nucleotide numbering starts with the first nucleotide of the R region, which corresponds to nt 375 in the HTLV-1 reference ATK sequence.

the 3′ end of all plus-strand viral transcripts (4, 13). This interaction is needed to overcome the negative effects of *cis*-acting repressive sequences (CRS) that promote nuclear retention and/or mRNA degradation. To date, CRS have been mapped within the

gag-pro-pol and *env* regions (14, 15) and in the R/U5 region of the long terminal repeat (LTR) (16). In some experimental systems, the RXRE, which overlaps the 3′ R region, was also shown to act as a CRS in the absence of Rex (15). The ability of Rex to rescue

TABLE 1 Sequences of primers and probe

Primer or probe	Sequence
3′-CRS s	5′-AGTAAGCTTCAGCAGGTCCTCCGGGCA-3′
3′-CRS as	5′-AGTAAGCTTCTGATAATAAGCATGGTTAACTT-3′
RXRE s	5′-AGTTCTAGACATGGCACGCATATGGCTC-3′
RXRE as	5′-AGTTCTAGACGATCTGTAACGGCGCAG-3′
pSG5E Δ5′SS s	5′-AGAACTTCAGGATGAGTTTGGG-3′
pSG5E Δ5′SS as	5′-CCCAAACTCATCCTGAAGTTCT-3′
beta globin intron s	5′-TAACCATGTTCATGCCTTCTTC-3′
beta globin as	5′-CCTATAGTGAGTCGTATTACAA-3′
beta globin probe	5′-(FAM)-CTGGTTATTGTGCTGTCTCATCATTTTG-(TAMRA)-3′
5′ promoter-SHAPE	5′-GCGCGCTAATACGACTCACTATAGGGCGGCCGCGGCTTTCCTCTTC-3′
3′-SHAPE	5′-CCTACTGGCCACCTGTCCAGATCGATCCGGTTCGCCGGATCCAAATCGGGCTTCGGTCCGGTTC-3′

RXRE-containing mRNAs relies on its binding to the nuclear export factor CRM1/exportin 1 (17). This interaction enhances nuclear export (18), thus subtracting the intron-containing mRNAs from the splicing machinery. Consistent with this model, Rex increases cytoplasmic levels of unspliced *gag-pro-pol* and singly spliced *env* mRNAs and decreases the production of the doubly spliced *tax/rex* mRNA (19). Other studies indicated that Rex might also act by inhibiting intron excision (20).

An additional layer of regulation at the posttranscriptional level is provided by p30Tof, a nucleolar/nuclear nonshuttling protein (21) that inhibits the nuclear export of the *tax/rex* mRNA, resulting in global inhibition of viral gene expression (22, 23). p30Tof also interacts with the RNA-binding domain of Rex and inhibits Rex-RXRE interaction (24). *hbz* transcripts do not contain the RXRE sequence and are therefore predicted to be Rex independent.

An investigation of the relationship between Rex function and the temporal pattern of viral expression in peripheral blood mononuclear cells (PBMCs) from infected patients (25) showed that HTLV-1 mRNAs are expressed with a two-phase kinetics in which Rex is critical to mediate a switch to late transcripts. Interestingly, in analogy with *gag-pro-pol* and *env*, the mRNAs for *p12/8*, *p13*, and *p30tof* were expressed in the late phase (25), suggesting that their expression might also be controlled by Rex. A similar "late" pattern of expression was observed for two multiply spliced mRNAs that encode functional Rex isoforms, Rex$_b$ and Rex$_c$ (9) (Fig. 1).

In the present study, we explored the effect of Rex on nucleocytoplasmic partitioning of transcripts coding for all of the viral proteins. The alternatively spliced mRNAs were detected using splice site-specific quantitative reverse transcription (qRT)-PCR, which allows discrimination between mRNAs of similar sizes and partially overlapping sequences. We found that expression of *tax/rex*, *p21rex*, and the recently identified *tax$_a$/rex$_a$* mRNAs was independent of Rex, while the cytoplasmic export of the *gag*, *env*, *p30tof*, *p13*, *p12/8*, *rex$_b$*, and *rex$_c$* mRNAs required Rex. All the Rex-dependent mRNAs contained a 75-nucleotide region that formed a stable stem-loop structure and was capable of increasing the nuclear retention and degradation of a reporter mRNA in the absence of other viral sequences. In the absence of Rex, all the Rex-dependent mRNAs exhibited a reduced half-life compared to Rex-independent transcripts. Time course experiments using hydroxyurea (HU) or aphidicolin (APHI) to block cells in G$_1$/S indicated that the majority of the transcripts become less Rex dependent when cells undergo mitosis, suggesting that the role of Rex in

governing the 2-phase kinetics of viral expression (25, 26) is more critical in resting or slowly dividing cells than in rapidly proliferating cells.

MATERIALS AND METHODS

Cell culture. The HeLa cell line and its derivative, HLtat (27), were maintained in Dulbecco's modified Eagle's medium (DMEM) (Sigma-Aldrich) supplemented with 10% fetal calf serum (FCS) (Invitrogen), 100 units/ml penicillin, and 20 units/ml streptomycin. The HTLV-1-infected cell line C8166 (28) was maintained in RPMI 1640 medium (Sigma-Aldrich) supplemented with 10% FCS and penicillin-streptomycin. Cells were synchronized by treatment with 0.5 mM hydroxyurea or with 0.75 mM aphidicolin (Sigma-Aldrich) (see the legend to Fig. 8). RNA half-lives were estimated by measuring the fraction remaining after treatment with actinomycin D (Sigma-Aldrich) to block transcription (1 μg/ml for HeLa cells and 5 μg/ml for C8166 cells); drug expulsion by the multidrug resistance pump was inhibited using 20 μg/ml verapamil (Sigma-Aldrich).

The HeLa and C8166 cell lines were obtained from the Istituto Nazionale per la Ricerca sul Cancro, Genoa, Italy (IST), Data Bank for Biomedical Research; the HLtat cells were kindly provided by G. Pavlakis and B. Felber (National Cancer Institute at Frederick, Frederick, MD, USA).

Plasmids. Plasmid ACH, which contains the full-length HTLV-1 proviral genome, and plasmid ACH-Rex knockout (ACH-Rex KO) have been previously described (25, 29). The 3′ CRS and RXRE sequences were PCR amplified from ACH DNA using primers containing tails with a restriction site for HindIII (3′ CRS) or XbaI (RXRE). The 3′ CRS comprised HTLV-1 nucleotides (nt) 6875 to 6949, and the RXRE comprised nt 8213 to 8544 (corresponding to nt 7250 to 7324 and nt 8588 to 8922, respectively, in the reference ATK sequence [GenBank no. J02029.1]). PCR products were digested with the appropriate restriction enzyme and inserted into the eukaryotic expression plasmid pSG5E, which is identical to pSG5 (Agilent Technology) except that it contains a polylinker with additional restriction sites derived from pBluescript (Stratagene). The QuikChange site-directed mutagenesis kit (Stratagene) was used to introduce a point mutation (GT to AT) in the 5′ splice site of the beta globin intron present in pSG5E. Primer sequences are listed in Table 1.

Transfections. HeLa and HLtat cells were seeded into 100-mm cell culture plates at 6 × 10^5 cells/plate and transfected 1 day later with 4 μg of plasmid DNA. Transfections were carried out using GeneJuice (Novagen), following the manufacturer's recommendations.

RNA extraction and qRT-PCR. Protocols for RNA isolation and qRT-PCR were described in detail previously (25, 30). Cytoplasmic and nuclear RNAs were isolated using the Paris kit (Ambion). The quality of the nuclear/cytoplasmic fractionation was assessed by measuring the partitioning of the 47S rRNA precursor using an Agilent Bioanalyzer (30). Total RNA was isolated using TRIzol (Invitrogen). RNA (1 μg) was treated with

DNase (Invitrogen) and reverse transcribed using SuperScript II reverse transcriptase (Invitrogen) and random hexamers, or a specific primer in the case of *hbz*. qRT-PCR was performed using primers and probes specific for individual transcripts. The normalized copy number (NCN) of each transcript in the cytoplasmic and nuclear fractions was determined by dividing the copy numbers of the individual HTLV-1 transcripts by the copy number of the glyceraldehyde-3-phosphate dehydrogenase (GAPDH) mRNA in the corresponding fraction. The export ratio of each transcript was calculated as follows: export ratio = NCN in the cytoplasmic fraction/(NCN in the cytoplasmic fraction + NCN in the nuclear fraction). Primer and probe sequences are listed in Table 1.

SHAPE. A DNA template for *in vitro* transcription was prepared by PCR amplification from the HTLV-1 ACH molecular clone using primers to introduce a T7 promoter at the 5′ end and a structure cassette for selective 2′-hydroxyl acylation analyzed by primer extension (SHAPE) at the 3′ end (Table 1) and Invitrogen Platinum High Fidelity *Taq* DNA polymerase. RNA was synthesized with the Ambion T7-Megascript kit, following the manufacturer's protocol. RNA was purified from denaturing 8 M urea-5% polyacrylamide gels, followed by elution and ethanol precipitation. The purified RNA was dissolved in sterile water.

Aliquots of RNA (20 pmol) were heated at 90°C for 3 min and snap cooled to 4°C. The volume was adjusted to 150 µl in 50 mM Tris-HCl (pH 8.0), 100 mM NaCl, 5 mM MgCl$_2$. Samples were incubated at 37°C for 15 min. The folded RNA was divided into two equal portions (72 µl) and treated with 8 µl of 25 mM 1-methyl-7-nitroisatoic anhydride (1M7) in anhydrous DMSO or DMSO alone. Samples were incubated at 37°C for 5 min, and RNA was precipitated at −20°C with 60 ng/µl glycogen, 0.3 M sodium acetate, pH 5.2, and 3 volumes of cold ethanol. The precipitated RNA was collected by centrifugation, washed once in 70% ethanol, and resuspended in 10 µl of water. The RNA was annealed to primers in 7-µl reaction mixtures at 85°C for 1 min, 60°C for 5 min, and 35°C for 5 min. 1M7-modified samples were annealed with 8 pmol of Cy5-labeled primer, and unmodified samples were annealed with 10 pmol of Cy5.5-labeled primer. The RNA was reverse transcribed at 50°C for 40 min with 100 U reverse transcriptase (Invitrogen Superscript III), 1× RT buffer (Invitrogen), 5 mM dithiothreitol (DTT), and 500 mM deoxynucleoside triphosphates (dNTPs) (Promega). The RNA was hydrolyzed with 200 mM NaOH for 5 min at 95°C, and the reactions were neutralized by adding HCl to 200 mM. Sequencing ladders were prepared using the Epicentre cycle-sequencing kit according to the manufacturer's instructions with primers labeled with WellRed D2 and LicorIR-800 dyes. Modified and control samples were mixed with the sequencing ladders, precipitated as described above, dried, and resuspended in 40 µl deionized formamide. Primer extension products were analyzed on a Beckman CEQ8000 Genetic Analysis System as described previously (31). Electropherograms were processed using the SHAPEfinder program, according to the software developer's protocol and included precalibration for matrixing and mobility shift for each set of primers as described previously (32, 33). Briefly, the area under each negative peak was subtracted from that of the corresponding positive peak. The resulting peak area difference at each nucleotide position was then divided by the average of the highest 8% of peak area differences after discounting any results greater than the 3rd quartile plus 1.5 times the interquartile range. Normalized intensities were introduced into RNA structure version 5.3 (34).

Cell cycle analyses. Cells were collected by trypsin treatment, centrifuged, and rinsed in phosphate-buffered saline (PBS). The cells were resuspended in 0.5 ml complete DMEM plus 0.5 ml FCS and fixed by adding 3 ml 70% ice-cold ethanol. After incubation at −20°C for 30 min, the cells were washed twice with PBS and incubated with 25 µg/ml propidium iodide and 0.5 µg/ml RNase A prepared in PBS at 37°C for 2 h. The cells were then analyzed with a FACSCalibur flow cytometer (BD Coulter) using the FL2-A channel to detect propidium iodide. DNA content frequency histograms were deconvoluted by using MODFIT LT software (Verity).

FIG 2 Rex dependence of HTLV-1 transcripts. (A) Export ratios of HTLV-1 mRNAs in HLtat cells harvested 24 h after transfection with ACH wild type (WT) or ACH-Rex KO. The bars represent mean values from 6 independent experiments with standard errors. The asterisks indicate a statistically significant difference (Mann-Whitney rank sum test; **, $P \leq 0.03$; ***, $P \leq 0.002$). (B) Export ratios of HTLV-1 mRNAs 24 h after transfection of HLtat cells with ACH-Rex KO or ACH-Rex KO plus pcRex (45). Mean values from 5 independent experiments and standard errors are shown. NUC, nuclear fraction; CYT, cytoplasmic fraction.

RESULTS

Effects of Rex on the nuclear export of HTLV-1 mRNAs. To assess the impact of Rex on the expression of individual HTLV-1 mRNAs, we compared their expression in a HeLa-derived cell line transfected with the HTLV-1 molecular clone ACH or with a derivative whose Rex AUG was ablated (ACH-Rex KO) (25). Cells were harvested 24 h posttransfection for isolation of RNA in the cytoplasmic and nuclear fractions. qRT-PCR was used to determine the NCN of each mRNA in the nuclear and cytoplasmic fractions and to calculate the export ratio (see Materials and Methods).

As shown in Fig. 2A, the export ratios of the *gag, env, p12, p13*,

FIG 3 Half-lives of HTLV-1 mRNAs. (A) Genome structures of the three proviruses present in the C8166 cell line. The provirus shown at the top does not carry deletions but is defective for Rex function due to a mutation of codon 112 of Rex generating a stop codon (*) in exon 3. The other two proviruses carry deletions encompassing large portions of the genome between the *gag* and *env* genes, including the first exon of Rex and Tax (see boxes with gray lines) (28). (B) mRNA levels in the nuclear and cytoplasmic fractions were measured by qRT-PCR. The Rex-independent *tax/rex* and *p21rex* mRNAs were more efficiently exported to the cytoplasm than Rex-dependent *gag* and *env* mRNAs. The plot shows mean values from 3 independent experiments with standard errors. (C to E) The Rex-defective cell line C8166 was treated with 5 μg/ml actinomycin D to block transcription and harvested for total RNA after the indicated time points. The NCNs of the individual transcripts were measured by qRT-PCR. The fraction of RNA remaining at each time point was calculated by dividing the NCN measured for each mRNA at that time point by its NCN measured at time zero. Shown are mean values from 5 independent experiments with standard errors. The dotted lines indicate 50% of the RNA remaining.

FIG 4 Mapping of a potential *cis*-acting regulatory element (3′ CRS) controlling Rex dependence. Alignment of all Rex-dependent and -independent HTLV-1 mRNAs indicates a putative *cis*-acting regulatory element comprising nt 6875 to 6949 (3′ CRS [boxed]) present in all the Rex-dependent mRNAs and absent from the Rex-independent transcripts.

and *p30tof* mRNAs were reduced by more than 80% in cells expressing the ACH-Rex KO molecular clone compared to wild-type ACH. Interestingly, the recently described *rex_b* and *rex_c* mRNAs (9) also showed Rex-dependent nuclear export. In contrast, the *tax/rex*, *p21rex*, and *tax_a/rex_a* mRNAs were efficiently exported both in the presence and in the absence of Rex. As previously reported (25), the export ratio of the *hbz sp1* mRNA was very low regardless of the presence of Rex. Cotransfection of a Rex expression plasmid with ACH-Rex KO substantially increased the

export ratio of the *gag*, *env*, *p12/p8*, *p13*, *p30tof*, *rex_b*, and *rex_c* mRNAs, thus confirming their Rex dependence (Fig. 2B). These findings are consistent with our previous observations identifying these transcripts as "late" mRNAs (9, 25). Interestingly, some transcripts were highly dependent on Rex (e.g., *gag*, *p13*, and *env*), while others (e.g., *p12/p8* and *rex_c*) were less Rex dependent, suggesting that the expression of the different transcripts is graded rather than an all-or-nothing phenomenon.

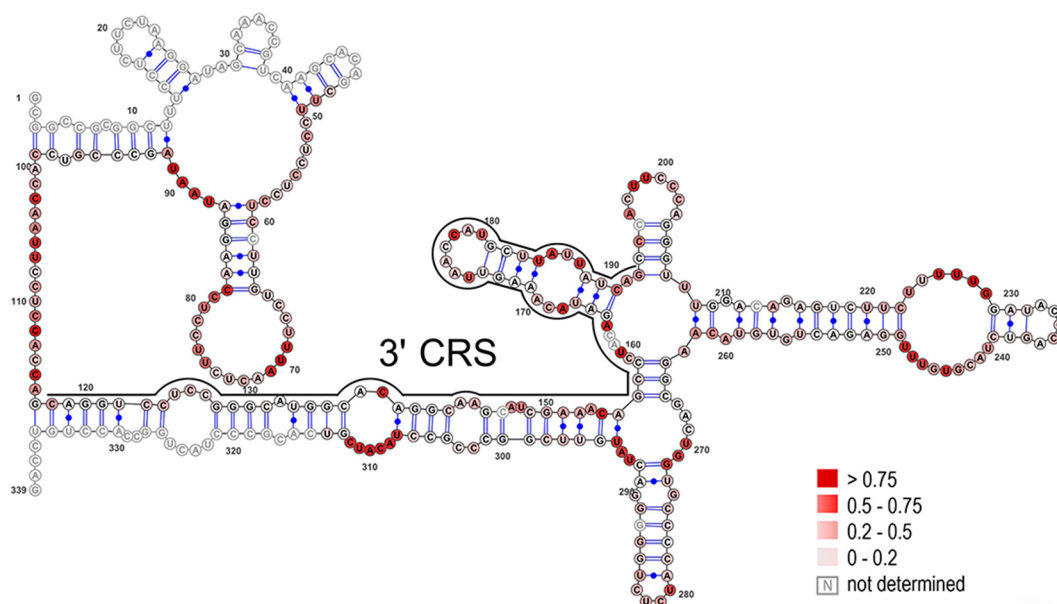**Reduced stability of Rex-dependent mRNAs.** We next tested

FIG 5 Secondary-structure model of the 3′ CRS RNA based on SHAPE folding. The nucleotides are color coded according to SHAPE reactivities using the scale provided. The 75-nt 3′ CRS sequence is indicated by the black trace.

whether, in the absence of Rex, Rex-dependent mRNAs are less stable than the Rex-independent mRNAs. To this end, we employed qRT-PCR to measure the fraction of mRNAs remaining following inhibition of RNA synthesis with actinomycin D. These experiments were performed in the T-cell line C8166, which contains three Rex-defective HTLV-1 proviruses (Fig. 3A and B) (28).

Our analysis showed that the doubly spliced Rex-independent *tax/rex* and *tax_a/rex_a* mRNAs had half-lives of approximately 8 h, while the Rex-dependent *p30tof*, *rex_b*, and *rex_c* mRNAs had half-lives of about 1 h (Fig. 3C). Among the singly spliced mRNAs (Fig. 3D), *p21rex* exhibited a half-life of 8 h, *p13* 4 h, *env* 1 h, and *p12/p8* less than 1 h. The unspliced *gag* mRNA also showed a half-life of less than 1 h (Fig. 3D). The *hbz sp1* mRNA exhibited a half-life of about 1 h (Fig. 3E), which is consistent with a recent study by Mocquet et al. (35).

Mapping a *cis*-acting element determining Rex responsiveness of HTLV-1 mRNAs. The experiments described above indicated that the *p12/8*, *p13*, *p30tof*, *rex_b*, and *rex_c* mRNAs required Rex for efficient nuclear export and stability. However, unlike *gag* and *env* mRNAs, these transcripts do not contain any of the previously identified *cis*-acting inhibitory sequences (see the introduction).

We thus hypothesized that a novel *cis*-acting regulatory sequence might determine their Rex dependence. Alignment of the sequences of all the mRNAs revealed a 75-nucleotide region between splice acceptors C and 3 (Fig. 4, boxed area) that is unique to Rex-dependent transcripts (*p12/p8*, *p13*, *p30tof*, *gag*, *env*, *rex_b*, and *rex_c*) but spliced out from the Rex-independent transcripts (*p21rex*, *tax/rex*, and *tax_a/rex_a*). We named this sequence the 3′ CRS.

SHAPE analysis of the 3′ CRS indicates that it folds into a stable stem-loop structure. To gain insight into the structure of the 3′ CRS, we employed SHAPE using a 339-nt RNA corresponding to nucleotide positions 6758 to 7097 of the of HTLV-1 genome; this region includes the 3′ CRS flanked by the 5′ intronic region (117 nt) and the exon 3 splice site (147 nt).

The SHAPE technique provides information on RNA structure at the individual nucleotide level using the selective chemical modification of the RNA backbone in structurally flexible regions. Our SHAPE protocol employed 1M7, which forms adducts on the 2′-hydroxyl groups, preferentially on unpaired nucleotides. Adduct formation was analyzed by primer extension and comparison of the resulting fragments with those from an unmodified control (see Materials and Methods).

Figure 5 shows a secondary-structure model based on SHAPE-constrained folding, with the normalized SHAPE reactivity for each nucleotide color coded and the 75-nt 3′ CRS sequence indicated by a black line. The model consists of a stem-loop structure formed by the 5′ intronic sequences and a second, more complex stem-loop structure that comprises the 3′ CRS and sequences spanning exon 3. Although we could not obtain data for the last 25 nt of the 339-nt RNA, the extended stem indicated in the model is probable, since it is also predicted by *in silico* folding of the 339-nt sequence performed using RNAfold (http://rna.tbi.univie.ac.at/cgi-bin/RNAfold.cgi) (data not shown). A recurring domain observed both *in silico* and in SHAPE is the stem-loop encompassing nucleotides 47 to 73 of the 75-nt 3′ CRS, suggesting that this region might provide a docking site for RNA-binding proteins controlling mRNA transport and stability.

Sequence comparison of the 3′ CRS in HTLV-1 proviruses from infected individuals. To identify a possible association between sequence variation of the 3′ CRS and the proviral load or clinical outcome of HTLV-1-infected individuals, we aligned the nucleotide sequence of the region in proviruses identified in a cohort of 86 patients with clinical manifestations and 34 healthy carriers (36) (Fig. 6A).

Sequence alignment using the ClustalW software revealed a high degree of conservation of the 3′ CRS, with one main recurrent A/G polymorphism at position 6901 (Fig. 6B, arrow). Complete clinical data and proviral-load information were available for 89 of the individuals. No apparent association was observed between the A/G polymorphism and clinical status (data not
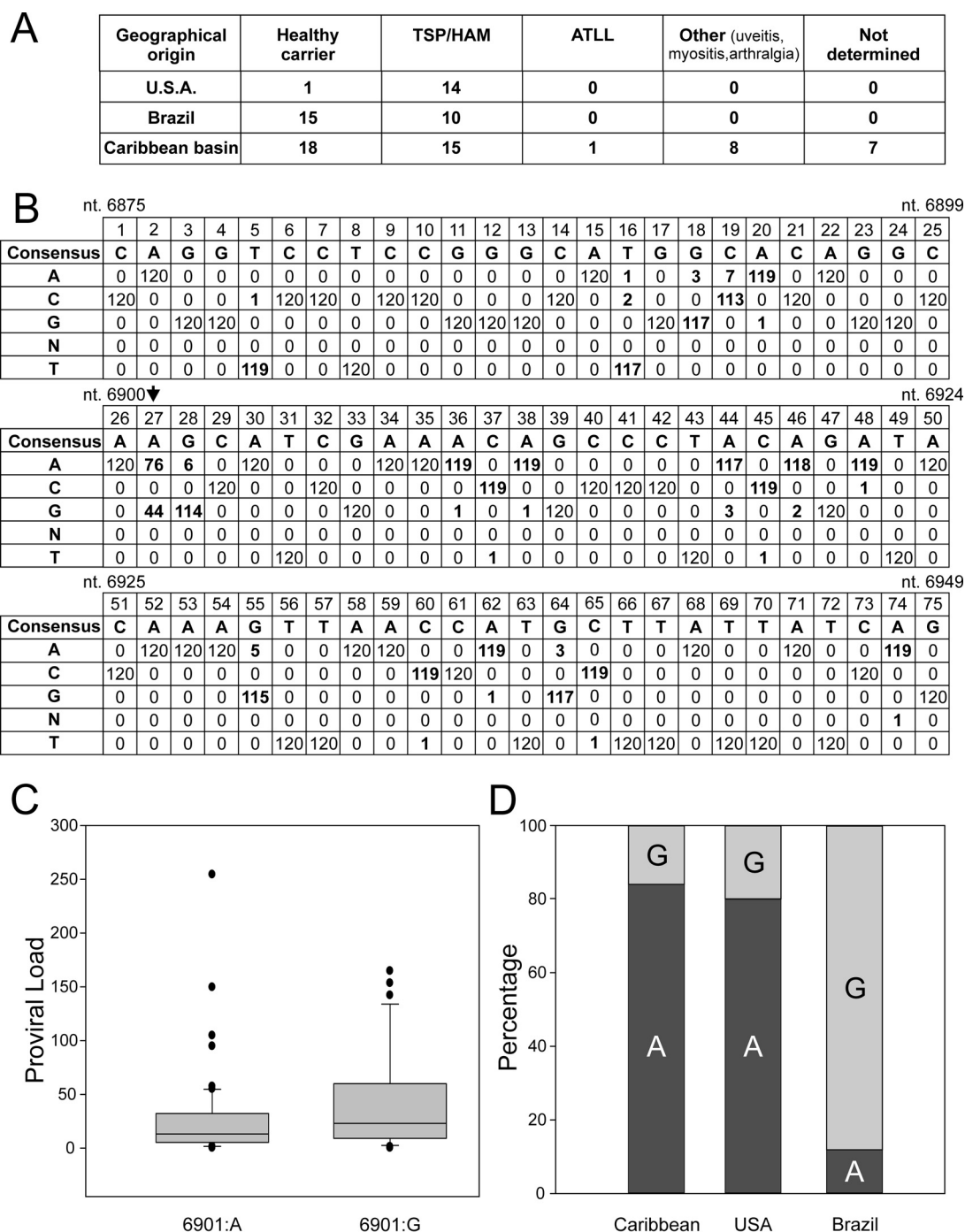
A

Geographical origin	Healthy carrier	TSP/HAM	ATLL	Other (uveitis, myositis,arthralgia)	Not determined
U.S.A.	1	14	0	0	0
Brazil	15	10	0	0	0
Caribbean basin	18	15	1	8	7

B

nt. 6875 — nt. 6899

	1	2	3	4	5	6	7	8	9	10	11	12	13	14	15	16	17	18	19	20	21	22	23	24	25
Consensus	C	A	G	G	T	C	C	T	C	C	G	G	G	C	A	T	G	G	C	A	C	A	G	G	C
A	0	120	0	0	0	0	0	0	0	0	0	0	0	0	120	1	0	3	7	119	0	120	0	0	0
C	120	0	0	0	1	120	120	0	120	120	0	0	0	120	0	2	0	0	113	0	120	0	0	0	120
G	0	0	120	120	0	0	0	0	0	0	120	120	120	0	0	0	120	117	0	1	0	0	120	120	0
N	0	0	0	0	0	0	0	0	0	0	0	0	0	0	0	0	0	0	0	0	0	0	0	0	0
T	0	0	0	0	119	0	0	120	0	0	0	0	0	0	0	117	0	0	0	0	0	0	0	0	0

nt. 6900▼ — nt. 6924

	26	27	28	29	30	31	32	33	34	35	36	37	38	39	40	41	42	43	44	45	46	47	48	49	50
Consensus	A	A	G	C	A	T	C	G	A	A	A	C	A	G	C	C	C	T	A	C	A	G	A	T	A
A	120	76	6	0	120	0	0	0	120	120	119	0	119	0	0	0	0	0	117	0	118	0	119	0	120
C	0	0	0	120	0	0	120	0	0	0	0	119	0	0	120	120	120	0	0	119	0	0	1	0	0
G	0	44	114	0	0	0	0	120	0	0	1	0	1	120	0	0	0	0	3	0	2	120	0	0	0
N	0	0	0	0	0	0	0	0	0	0	0	0	0	0	0	0	0	0	0	0	0	0	0	0	0
T	0	0	0	0	0	120	0	0	0	0	0	1	0	0	0	0	0	120	0	1	0	0	0	120	0

nt. 6925 — nt. 6949

	51	52	53	54	55	56	57	58	59	60	61	62	63	64	65	66	67	68	69	70	71	72	73	74	75
Consensus	C	A	A	A	G	T	T	A	A	C	C	A	T	G	C	T	T	A	T	T	A	T	C	A	G
A	0	120	120	120	5	0	0	120	120	0	0	119	0	3	0	0	0	120	0	0	120	0	0	119	0
C	120	0	0	0	0	0	0	0	0	119	120	0	0	0	119	0	0	0	0	0	0	0	120	0	0
G	0	0	0	0	115	0	0	0	0	0	0	0	0	117	0	0	0	0	0	0	0	0	0	0	120
N	0	0	0	0	0	0	0	0	0	0	0	0	0	0	0	0	0	0	0	0	0	0	0	1	0
T	0	0	0	0	0	120	120	0	0	1	0	0	120	0	1	120	120	0	120	120	0	120	0	0	0

C — Boxplot of Proviral Load (y-axis 0–300) for groups 6901:A and 6901:G.

D — Bar chart of Percentage (y-axis 0–100) showing A/G proportions for Caribbean, USA, and Brazil (A = dark, G = light).

FIG 6 Sequence polymorphism in the 3′ CRS in proviruses from HTLV-1-infected subjects. (A) Geographical origins and clinical findings for HTLV-1-infected subjects. (B) Sequence alignment of the 3′ CRS in a cohort of 120 HTLV-1-infected subjects using ClustalW software. The numbers in the boxes are the numbers of HTLV-1-infected individuals with the corresponding nucleotide in that position. Nucleotide 6901 is indicated by the arrow. (C) Boxplots represent the proviral load of subjects infected with HTLV-1 strains carrying one of the two polymorphic variants in the 3′-CRS at position 6901 (*t* test; *P* value = 0.069). The lines in the middle of the boxplots represent median values, while the tops and bottoms of the boxplots represent the 25th and 75th percentile; whiskers (error bars) above and below the boxes indicate the 90th and 10th percentiles. Outlier samples are represented as dots out of whisker limits. (D) Percentages of subjects from different geographical areas with A or G at position 6901. Nucleotide 6901 corresponds to nt 7276 in the ATK reference sequence.

shown) or proviral load (Fig. 6C). However, the polymorphism seemed to be strongly associated with the geographical origin of the individuals, with the A variant identified in the majority of subjects from the Caribbean basin and United States, while G prevailed in Brazilian individuals (Fig. 6D). Taken together, these findings suggest that the 3′ CRS sequence is highly conserved and that the A/G polymorphism is not likely to affect the overall propagation of the virus or its pathogenic properties.

Activity of the 3′ CRS in a heterologous reporter system. To gain insight into the function of the 3′ CRS, we next tested
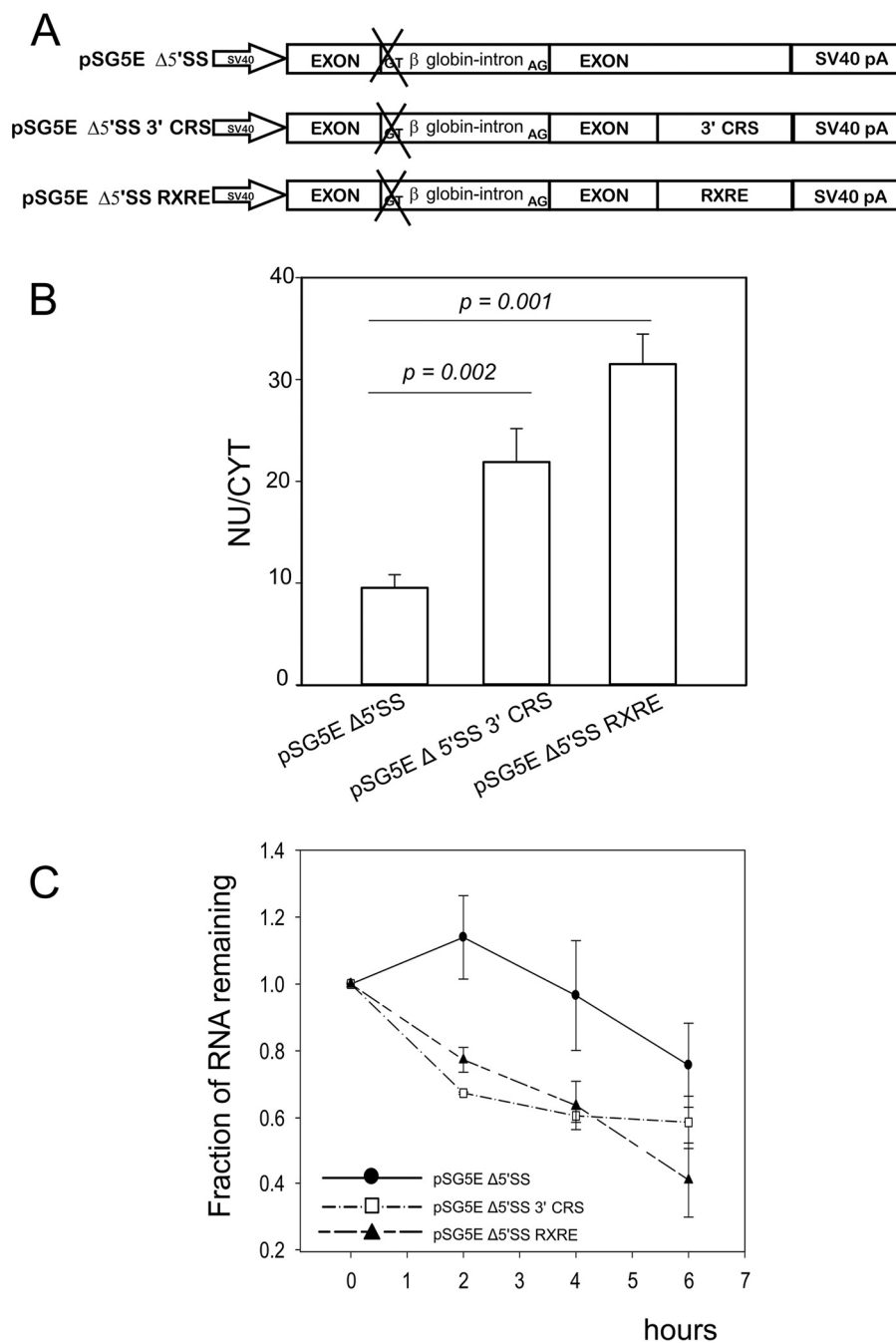
FIG 7 Functional characterization of the 3′ CRS sequence. (A) Schematic representation of the reporter constructs used to test the effects of the 3′ CRS on mRNA export and stability. "X" indicates mutation of the 5′ SS from GT to AT. (B) Effects of the 3′ CRS on nuclear retention. HeLa cells were synchronized for 16 h using HU, released from the block by washing out the HU, transfected 6 h later with the reporter plasmids, and harvested 16 h after transfection. The graph shows the mean ratios between the NCNs in the nuclear and cytoplasmic fractions measured in 7 independent experiments with standard errors. The P values were calculated with the Mann-Whitney rank sum test. (C) Half-lives of reporter mRNAs containing the 3′ CRS or RXRE. HeLa cells were transfected as described above. Sixteen hours after transfection, actinomycin D (1 μg/ml) was added to block transcription, and cells were harvested for total RNA extraction after 0, 2, 4, or 6 h of incubation. The fraction of reporter RNA remaining at each time point was calculated as described in the legend to Fig. 3. The graph shows mean values from 3 independent experiments with standard errors.

whether it affected the nucleocytoplasmic transport and/or the stability of a heterologous reporter mRNA lacking HTLV-1 sequences. As depicted in Fig. 7A, the 3′ CRS was inserted into an expression plasmid derived from pSG5, between the beta-globin intron and the simian virus 40 (SV40) polyadenylation signal/site.

This reporter was similar to a construct employed in earlier studies of HIV Rev, which indicated that Rev dependence requires the presence of an inefficient 5′ or 3′ splice site to mimic the relative inefficiency of viral splice sites compared to cellular splice sites (37). We therefore mutated the 5′ splice site of the beta-globin

intron from GT to AT. A control reporter plasmid contained the RXRE, which can act as a nuclear retention sequence in the absence of Rex (15). The resulting constructs (Fig. 7A) were transfected into HeLa cells that had been synchronized using HU block-release. Sixteen hours posttransfection, cells were harvested and qRT-PCR was performed to quantify unspliced reporter RNA in the nuclear and cytoplasmic compartments. These experiments (Fig. 7B) revealed that the presence of the 3′ CRS in the reporter RNA significantly increased its nuclear retention (calculated as the nuclear NCN/cytoplasmic NCN ratio). This effect of the 3′ CRS was statistically significant and comparable to that of the RXRE.

To determine the influence of the 3′ CRS on the stability of the reporter RNA, transfected cells were treated with actinomycin D and harvested at different time points, as described above. This analysis revealed that the 3′ CRS-containing transcript was less stable than the control mRNA (Fig. 7C). This destabilizing effect of the 3′ CRS was comparable to that of the RXRE.

Effects of cell division on HTLV-1 mRNA expression. The findings described above are consistent with the temporal pattern of viral genes described in our previous studies (9, 25) (i.e., intermediate-late temporal for *p30tof*, *p13*, *p12/8*, *rex_b*, and *rex_c* and early for *p21rex* and *tax_a/rex_a*). However, in a recent study carried out in the cell line 293T, Li et al. observed that expression of *p13*, *p21rex*, *p12/p8*, and *p30tof* mRNAs is not affected by Rex (38). Considering the high proliferation index of 293T cells and the longer time frame of the experiments performed by these authors (48 h), we surmised that the Rex independence of the *p13*, *p12/8*, and *p30tof* mRNAs might be due to their release into the cytoplasm following disassembly of the nuclear envelope during mitosis.

In fact, when we carried out our experiments in the HeLa-derived cell line for a more prolonged time (i.e., harvesting 48 h after transfection), we observed a consistent increase in the export ratios of the Rex-dependent mRNAs expressed by the ACH-Rex KO molecular clone (Fig. 8A).

To directly test the role of mitosis in this phenomenon, we synchronized the cells by treating them with HU, which inhibits ribonucleotide reductase, resulting in a block in the G_1 phase of the cell cycle. As shown in Fig. 8B, cells were exposed to hydroxyurea (HU) for 16 h, after which the HU was washed out; the cells were then allowed to recover for 6 h, transfected with ACH-Rex KO, and divided into three replicate cultures, one of which was cultured for an additional 18 h (a period too brief for most cells to undergo mitosis). A second set was cultured for 42 h after transfection in order to permit cell division [long culture (mitosis)], and the third replicate was subjected to a second HU block 18 h after transfection to prevent mitosis and then harvested at 42 h [long culture + drug (no mitosis)]. Cell cycle analysis (Fig. 8C) of cultures harvested at different time points of the experiment confirmed that the first HU treatment arrested the cells at the G_1-S checkpoint (point 2); the cells were in S phase at the time of transfection (point 3), and the short culture (point 4) and the long culture plus HU (point 6) contained fewer cells in G_2/M than the untreated long culture (point 5).

Comparison of export ratios measured at the 18-hour short-culture (Fig. 8D, black bars) and 42-hour long-culture (green bars) time points confirmed that prolonging the incubation time to allow mitosis favored nuclear export of Rex-dependent mRNAs. However, this effect was abrogated in cells that were subjected to the second HU block (red bars), indicating that release of the transcripts into the cytoplasm depended on whether the cells

were allowed to undergo mitosis. This mitosis-dependent release appeared to be unequal for the different transcripts: the *p13*, *p30tof*, and *env* mRNAs were absent from the cytoplasm at the early postblock time point and at the long-culture plus HU time point, while a more partial effect was observed for *gag*, *p12/8*, and *rex_b*, and little or no effect for *rex_c* (Fig. 8D). These observations suggest that different transcripts might be more or less tightly confined in the nuclear compartment in the absence of either Rex or mitosis.

To reinforce these observations, we performed additional experiments using aphidicolin (APHI), which inhibits DNA polymerases α and δ, resulting in a block in S phase. As shown in Fig. 8E, cells were exposed to APHI for 24 h, after which the drug was washed out and the cells were transfected with ACH-Rex KO and divided into three replicate cultures, one of which was cultured for an additional 12 h. A second set was cultured for 36 h after transfection in order to permit cell division [long culture (mitosis)], and the third replicate was subjected to a second APHI block 12 h after transfection to prevent mitosis and then harvested at 36 h [long culture + drug (no mitosis)]. The results of cell cycle analysis (Fig. 8F) confirmed that the majority of the cells were in S phase at the time of transfection (point 2) and that the short culture (point 3) and the long culture plus APHI (point 5) contained fewer cells in G_2/M than the untreated long culture (point 4).

Similar to results obtained with HU, the APHI-synchronized cells showed a progressive increase in the cytoplasmic export of Rex-dependent transcripts, which was abrogated by the second APHI block in the case of the *gag*, *env*, *p13*, *p30tof*, and *p12/p8* mRNAs (Fig. 8F). Overall, the levels of cytoplasmic Rex-dependent transcripts measured at the early postblock time point were higher in APHI-treated cells than in HU-treated cells, a difference that may reflect the degree of synchronization obtained with the two drugs (compare Fig. 8C and F, left).

Taken together, the results obtained with the HU and APHI blocks indicated that most transcripts become less Rex dependent when cells undergo mitosis. This finding suggests that the ability of Rex to determine the 2-phase kinetics of viral gene expression (25, 26) may be especially pronounced in resting or slowly dividing cells.

DISCUSSION

In the present study, we investigated the Rex dependence and nucleocytoplasmic partitioning of the alternatively spliced HTLV-1 transcripts. The results obtained with wild-type and ACH-Rex KO HTLV-1 molecular clones confirmed previous studies of the *tax/rex*, *gag*, and *env* mRNAs and revealed that among the mRNAs coding for the accessory proteins, the *p21rex* and *tax_a/rex_a* mRNAs did not require Rex for efficient export, while the *p30tof*, *p13*, *p12/8*, *rex_b*, and *rex_c* mRNAs were Rex dependent (Fig. 2A and B). In addition to being retained in the nucleus, in the absence of Rex, these mRNAs had shorter half-lives than Rex-independent transcripts (Fig. 3).

The observation that the *tax/rex* mRNA is Rex independent is consistent with the results of several previous studies (19, 38–41) that examined expression of viral transcripts from the complete provirus. However, studies based on expression of intronless mature mRNAs showed that expression of *tax/rex*, as well as other viral transcripts, may be enhanced by Rex through a canonical RXRE- and CRM1-dependent pathway (42, 43). In fact, Rex is capable of binding *tax/rex* mRNA in chronically infected cell lines
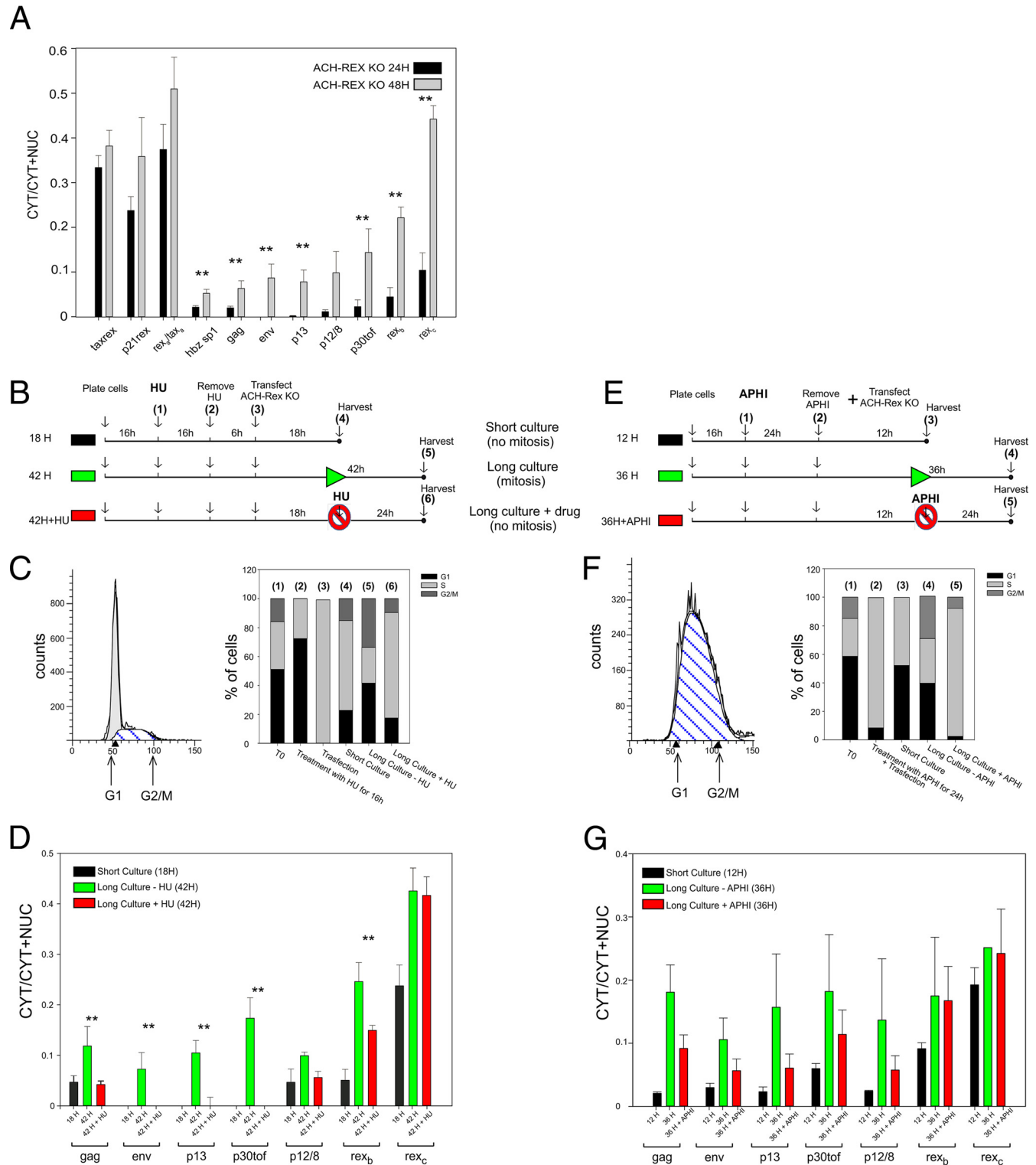
FIG 8 Effects of mitosis on HTLV-1 mRNA expression. (A) Export ratios of HTLV-1 mRNAs 24 h or 48 h after transfection of HLtat cells with ACH-Rex KO. Mean values from 4 independent experiments and standard errors are shown. The asterisks indicate a statistically significant difference (Mann-Whitney rank sum test; **, $P < 0.05$). (B) HLtat cells were synchronized using HU, released from the block, and transfected with ACH-Rex KO. (C) (Left) Cells following the first block with HU. (Right) Phase distribution of the cells corresponding to each step (1 to 6) of the experiment. (D) Export ratios of HTLV-1 mRNAs were measured 18 h or 42 h after transfection in the absence ($-$) or presence ($+$) of a second HU block for the final 24 h. Mean values from 5 independent experiments and standard errors are shown. The asterisks indicate a statistically significant difference with a Mann-Whitney rank sum test (**, $P \leq 0.03$). (E) HLtat cells were synchronized with APHI, released from the block, and transfected with ACH-Rex KO. (F) (Left) Cells following the first block with APHI. (Right) Phase distribution of the cells corresponding to each step (1 to 5) of the experiment. (G) Export ratios of HTLV-1 mRNAs were measured 12 h or 36 h after transfection in the absence or presence of a second APHI block for the final 24 h. Mean values from 3 independent experiments and standard errors are shown.

(43). The distinct observations made from a study of full-length proviruses versus mRNAs produced from cDNA expression plasmids indicate that the latter may be subjected to additional expression constraints that are not encountered by transcripts that interact with the splicing machinery.

Our findings also revealed a 75-nucleotide region (3′ CRS) in all Rex-dependent mRNAs that is absent from those that are Rex independent (Fig. 4). Sequence analysis of the 3′ CRS in proviruses from HTLV-1-infected subjects revealed a high degree of conservation (Fig. 6). The 3′ CRS sequence increased nuclear retention and degradation of a reporter mRNA in the absence of other viral sequences, suggesting its role as a *cis*-acting inhibitory element. The stable hairpin structure in the 3′ CRS revealed by SHAPE (Fig. 5) suggests that, analogous to other highly structured regions in viral mRNAs, the 3′ CRS might be associated with regulatory functions by providing a docking site(s) for RNA-binding proteins.

Our findings are consistent with the intermediate-late temporal pattern of expression of the *p30tof*, *p13*, *p12/8*, *rex*$_b$, and *rex*$_c$ mRNAs described in our previous studies (9, 25) based on the *ex vivo* reactivation of primary cells isolated from HTLV-1-infected patients; in contrast, *p21rex* and *tax*$_a$/*rex*$_a$ were expressed as early genes, supporting their Rex independence (9, 25). On the other hand, our observations in part contradict the results of a recent study by Li et al. that showed that expression of the *p13*, *p21rex*, *p12/p8*, and *p30tof* mRNAs is not affected by Rex in 293T cells (38). Considering the higher proliferation index of 293T cells than of the HeLa-derived cell line that we used and the longer time frame of the experiments performed by Li et al. (48 h) than in our experiments (24 h), we propose that the Rex independence of the *p13*, *p12/8*, and *p30tof* mRNAs observed by those authors reflects the release of the mRNAs into the cytoplasm following disassembly of the nuclear envelope during mitosis. This hypothesis was supported by the observation that, in our experimental system, cultivation of the transfected cells for a time that exceeds their division time resulted in a significant increase in the export ratios of the Rex-dependent transcripts in the absence of Rex (Fig. 8A). This effect could be explained by different mechanisms, e.g., that over time, putative factors that recognize the 3′ CRS become saturated with transcripts, thereby allowing free transcripts to leak out of the nucleus. However, the finding that inhibition of mitosis using hydroxyurea or aphidicolin resulted in a decrease in their export ratios after long incubation times strongly supports a role for mitosis in this phenomenon (Fig. 8B to G).

Collectively, our results suggest that control of HTLV-1 gene expression by Rex is partially lost during mitosis due to disassembly of the nuclear envelope. Studies on the regulation of HTLV-1 expression should therefore be carried out in experimental models that take into account the influence of cell division. Our findings also suggest that, in the natural viral life cycle, Rex function is likely to be critical in resting or slowly dividing cells, where it would determine the 2-phase kinetics of viral expression that was observed in previous studies (25, 26). A recent study by Philip et al. showed an association between a productive profile of infection and a cellular quiescent phenotype compatible with senescence (44). Interestingly, this condition was associated with high NF-κB, high Tax, and relatively low HBZ activity. Philip et al. also showed that HBZ inhibited Rex-mediated export of the *gag-pro-pol* and *env* mRNAs. Although these data were demonstrated in a different

cellular system than the one we employed, they lead us to hypothesize that the function of Rex in determining a 2-phase kinetics of viral expression would be particularly critical in this senescent population to temporally restrain the exposure of highly antigenic viral proteins (e.g., Tax, Gag, and Env), favoring escape of infected cells from immune recognition and promoting lifelong virus persistence. Our observations thus add a layer of complexity to the mechanisms controlling the expression of alternatively spliced HTLV-1 mRNAs and suggest a possible contribution of the cycling properties of the host cell to the pattern of viral gene expression and latency.

ACKNOWLEDGMENTS

FUNDING INFORMATION

REFERENCES

1. **Ishitsuka K, Tamura K.** 2014. Human T-cell leukaemia virus type I and adult T-cell leukaemia-lymphoma. Lancet Oncol **15**:e517–e526. http://dx.doi.org/10.1016/S1470-2045(14)70202-5.
2. **Yamano Y, Sato T.** 2012. Clinical pathophysiology of human T-lymphotropic virus-type 1-associated myelopathy/tropical spastic paraparesis. Front Microbiol **3**:389. http://dx.doi.org/10.3389/fmicb.2012.00389.
3. **Martin F, Taylor GP, Jacobson S.** 2014. Inflammatory manifestations of HTLV-1 and their therapeutic options. Expert Rev Clin Immunol **10**:1531–1546. http://dx.doi.org/10.1586/1744666X.2014.966690.
4. **Cavallari I, Rende F, D'Agostino DM, Ciminale V.** 2011. Converging strategies in expression of human complex retroviruses. Viruses **3**:1395–1414. http://dx.doi.org/10.3390/v3081395.
5. **Nagashima K, Yoshida M, Seiki M.** 1986. A single species of pX mRNA of human T-cell leukemia virus type I encodes trans-activator p40x and two other phosphoproteins. J Virol **60**:394–399.
6. **Ciminale V, Pavlakis GN, Derse D, Cunningham CP, Felber BK.** 1992. Complex splicing in the human T-cell leukemia virus (HTLV) family of retroviruses: novel mRNAs and proteins produced by HTLV type I. J Virol **66**:1737–1745.
7. **Koralnik IJ, Gessain A, Klotman ME, Lo Monico A, Berneman ZN, Franchini G.** 1992. Protein isoforms encoded by the pX region of human T-cell leukemia/lymphotropic virus type I. Proc Natl Acad Sci U S A **89**:8813–8817. http://dx.doi.org/10.1073/pnas.89.18.8813.
8. **Berneman ZN, Gartenhaus RB, Reitz MS, Jr, Blattner WA, Manns A, Hanchard B, Ikehara O, Gallo RC, Klotman ME.** 1992. Expression of alternatively spliced human T-lymphotropic virus type I pX mRNA in infected cell lines and in primary uncultured cells from patients with adult T-cell leukemia/lymphoma and healthy carriers. Proc Natl Acad Sci U S A **89**:3005–3009. http://dx.doi.org/10.1073/pnas.89.7.3005.
9. **Rende F, Cavallari I, Andresen V, Valeri VW, D'Agostino DM, Franchini G, Ciminale V.** 2015. Identification of novel monocistronic HTLV-1 mRNAs encoding functional Rex isoforms. Retrovirology **12**:58. http://dx.doi.org/10.1186/s12977-015-0184-2.
10. **Larocca D, Chao LA, Seto MH, Brunck TK.** 1989. Human T-cell leukemia virus minus strand transcription in infected T-cells. Biochem Biophys Res Commun **163**:1006–1013. http://dx.doi.org/10.1016/0006-291X(89)92322-X.
11. **Cavanagh MH, Landry S, Audet B, Arpin-Andre C, Hivin P, Pare ME, Thete J, Wattel E, Marriott SJ, Mesnard JM, Barbeau B.** 2006. HTLV-I

antisense transcripts initiating in the 3′LTR are alternatively spliced and polyadenylated. Retrovirology **3:**15. http://dx.doi.org/10.1186/1742-4690-3-15.

12. **Gaudray G, Gachon F, Basbous J, Biard-Piechaczyk M, Devaux C, Mesnard JM.** 2002. The complementary strand of the human T-cell leukemia virus type 1 RNA genome encodes a bZIP transcription factor that down-regulates viral transcription. J Virol **76:**12813–12822. http://dx.doi.org/10.1128/JVI.76.24.12813-12822.2002.

13. **Rende F, Cavallari I, Romanelli MG, Diani E, Bertazzoni U, Ciminale V.** 2012. Comparison of the genetic organization, expression strategies and oncogenic potential of HTLV-1 and HTLV-2. Leuk Res Treatment **2012:**876153. http://dx.doi.org/10.1155/2012/876153.

14. **Saiga A, Orita S, Minoura-Tada N, Maeda M, Aono Y, Asakawa M, Nakahara K, Kubota R, Osame M, Igarashi H.** 1997. cis-Acting inhibitory elements within the pol-env region of human T-cell leukemia virus type 1 possibly involved in viral persistence. J Virol **71:**4485–4494.

15. **King JA, Bridger JM, Lochelt M, Lichter P, Schulz TF, Schirrmacher V, Khazaie K.** 1998. Nucleocytoplasmic transport of HTLV-1 RNA is regulated by two independent LTR encoded nuclear retention elements. Oncogene **16:**3309–3316. http://dx.doi.org/10.1038/sj.onc.1201884.

16. **Seiki M, Hikikoshi A, Yoshida M.** 1990. The U5 sequence is a cis-acting repressive element for genomic RNA expression of human T cell leukemia virus type I Virology **176:**81–86.

17. **Hakata Y, Umemoto T, Matsushita S, Shida H.** 1998. Involvement of human CRM1 (exportin 1) in the export and multimerization of the Rex protein of human T-cell leukemia virus type 1. J Virol **72:**6602–6607.

18. **Nakano K, Watanabe T.** 2012. HTLV-1 Rex: the courier of viral messages making use of the host vehicle. Front Microbiol **3:**330. http://dx.doi.org/10.3389/fmicb.2012.00330.

19. **Hidaka M, Inoue J, Yoshida M, Seiki M.** 1988. Post-transcriptional regulator (rex) of HTLV-1 initiates expression of viral structural proteins but suppresses expression of regulatory proteins. EMBO J **7:**519–523.

20. **Grone M, Koch C, Grassmann R.** 1996. The HTLV-1 Rex protein induces nuclear accumulation of unspliced viral RNA by avoiding intron excision and degradation. Virology **218:**316–325. http://dx.doi.org/10.1006/viro.1996.0200.

21. **D'Agostino DM, Ciminale V, Zotti L, Rosato A, Chieco-Bianchi L.** 1997. The human T-cell lymphotropic virus type 1 Tof protein contains a bipartite nuclear localization signal that is able to functionally replace the amino-terminal domain of Rex. J Virol **71:**75–83.

22. **Nicot C, Dundr M, Johnson JM, Fullen JR, Alonzo N, Fukumoto R, Princler GL, Derse D, Misteli T, Franchini G.** 2004. HTLV-1-encoded p30(II) is a post-transcriptional negative regulator of viral replication. Nat Med **10:**197–201. http://dx.doi.org/10.1038/nm984.

23. **Younis I, Khair L, Dundr M, Lairmore MD, Franchini G, Green PL.** 2004. Repression of human T-cell leukemia virus type 1 and type 2 replication by a viral mRNA-encoded posttranscriptional regulator. J Virol **78:**11077–11083. http://dx.doi.org/10.1128/JVI.78.20.11077-11083.2004.

24. **Sinha-Datta U, Datta A, Ghorbel S, Dodon MD, Nicot C.** 2007. Human T-cell lymphotrophic virus type I rex and p30 interactions govern the switch between virus latency and replication. J Biol Chem **282:**14608–14615. http://dx.doi.org/10.1074/jbc.M611219200.

25. **Rende F, Cavallari I, Corradin A, Silic-Benussi M, Toulza F, Toffolo GM, Tanaka Y, Jacobson S, Taylor GP, D'Agostino DM, Bangham CR, Ciminale V.** 2011. Kinetics and intracellular compartmentalization of HTLV-1 gene expression: nuclear retention of HBZ mRNA. Blood **117:**4855–4859. http://dx.doi.org/10.1182/blood-2010-11-316463.

26. **Corradin A, Di Camillo B, Ciminale V, Toffolo G, Cobelli C.** 2011. Sensitivity analysis of retrovirus HTLV-1 transactivation. J Comput Biol **18:**183–193. http://dx.doi.org/10.1089/cmb.2010.0219.

27. **Schwartz S, Felber BK, Benko DM, Fenyo EM, Pavlakis GN.** 1990. Cloning and functional analysis of multiply spliced mRNA species of human immunodeficiency virus type 1. J Virol **64:**2519–2529.

28. **Bhat NK, Adachi Y, Samuel KP, Derse D.** 1993. HTLV-1 gene expression by defective proviruses in an infected T-cell line. Virology **196:**15–24. http://dx.doi.org/10.1006/viro.1993.1450.

29. **Kimata JT, Wong FH, Wang JJ, Ratner L.** 1994. Construction and characterization of infectious human T-cell leukemia virus type 1 molecular clones. Virology **204:**656–664. http://dx.doi.org/10.1006/viro.1994.1581.

30. **Cavallari I, Rende F, Ciminale V.** 2014. Quantitative analysis of human T-lymphotropic virus type 1 (HTLV-1) gene expression using nucleocytoplasmic fractionation and splice junction-specific real-time RT-PCR (qRT-PCR). Methods Mol Biol **1087:**325–337. http://dx.doi.org/10.1007/978-1-62703-670-2_26.

31. **Mitra S, Shcherbakova IV, Altman RB, Brenowitz M, Laederach A.** 2008. High-throughput single-nucleotide structural mapping by capillary automated footprinting analysis. Nucleic Acids Res **36:**e63. http://dx.doi.org/10.1093/nar/gkn267.

32. **Badorrek CS, Weeks KM.** 2006. Architecture of a gamma retroviral genomic RNA dimer. Biochemistry **45:**12664–12672. http://dx.doi.org/10.1021/bi060521k.

33. **Wilkinson KA, Gorelick RJ, Vasa SM, Guex N, Rein A, Mathews DH, Giddings MC, Weeks KM.** 2008. High-throughput SHAPE analysis reveals structures in HIV-1 genomic RNA strongly conserved across distinct biological states. PLoS Biol **6:**e96. http://dx.doi.org/10.1371/journal.pbio.0060096.

34. **Deigan KE, Li TW, Mathews DH, Weeks KM.** 2009. Accurate SHAPE-directed RNA structure determination. Proc Natl Acad Sci U S A **106:**97–102. http://dx.doi.org/10.1073/pnas.0806929106.

35. **Mocquet V, Neusiedler J, Rende F, Cluet D, Robin JP, Terme JM, Dodon MD, Wittmann J, Morris C, Le Hir H, Ciminale V, Jalinot P.** 2012. The human T-lymphotropic virus type 1 Tax protein inhibits nonsense-mediated mRNA decay by interacting with INT6/EIF3E and UPF1. J Virol **86:**7530–7543. http://dx.doi.org/10.1128/JVI.07021-11.

36. **Pise-Masison CA, de Castro-Amarante MF, Enose-Akahata Y, Buchmann RC, Fenizia C, Washington Parks R, Edwards D, Fiocchi M, Alcantara LC, Jr, Bialuk I, Graham J, Walser JC, McKinnon K, Galvao-Castro B, Gessain A, Venzon D, Jacobson S, Franchini G.** 2014. Co-dependence of HTLV-1 p12 and p8 functions in virus persistence. PLoS Pathog **10:**e1004454. http://dx.doi.org/10.1371/journal.ppat.1004454.

37. **Chang DD, Sharp PA.** 1989. Regulation by HIV Rev depends upon recognition of splice sites. Cell **59:**789–795. http://dx.doi.org/10.1016/0092-8674(89)90602-8.

38. **Li M, Kannian P, Yin H, Kesic M, Green PL.** 2012. Human T lymphotropic virus type 1 regulatory and accessory gene transcript expression and export are not rex dependent. AIDS Res Hum Retroviruses **28:**405–410. http://dx.doi.org/10.1089/aid.2011.0130.

39. **Inoue J, Itoh M, Akizawa T, Toyoshima H, Yoshida M.** 1991. HTLV-1 Rex protein accumulates unspliced RNA in the nucleus as well as in cytoplasm. Oncogene **6:**1753–1757.

40. **Inoue J, Seiki M, Yoshida M.** 1986. The second pX product p27 chi-III of HTLV-1 is required for gag gene expression. FEBS Lett **209:**187–190. http://dx.doi.org/10.1016/0014-5793(86)81108-5.

41. **Inoue J, Yoshida M, Seiki M.** 1987. Transcriptional (p40x) and post-transcriptional (p27x-III) regulators are required for the expression and replication of human T-cell leukemia virus type I genes. Proc Natl Acad Sci U S A **84:**3653–3657. http://dx.doi.org/10.1073/pnas.84.11.3653.

42. **D'Agostino DM, Ciminale V, Zotti L, Chieco-Bianchi L.** 1999. Influence of Rex and intronic sequences on expression of spliced mRNAs produced by human T cell leukemia virus type I. AIDS Res Hum Retroviruses **15:**1351–1363. http://dx.doi.org/10.1089/088922299310061.

43. **Bai XT, Sinha-Datta U, Ko NL, Bellon M, Nicot C.** 2012. Nuclear export and expression of human T-cell leukemia virus type 1 tax/rex mRNA are RxRE/Rex dependent. J Virol **86:**4559–4565. http://dx.doi.org/10.1128/JVI.06361-11.

44. **Philip S, Zahoor MA, Zhi H, Ho YK, Giam CZ.** 2014. Regulation of human T-lymphotropic virus type I latency and reactivation by HBZ and Rex. PLoS Pathog **10:**e1004040. http://dx.doi.org/10.1371/journal.ppat.1004040.

45. **Rimsky L, Hauber J, Dukovich M, Malim MH, Langlois A, Cullen BR, Greene WC.** 1988. Functional replacement of the HIV-1 rev protein by the HTLV-1 rex protein. Nature **335:**738–740. http://dx.doi.org/10.1038/335738a0.